Diffractive Production of Real Photons

D. Reyna [a] * †

[a]DESY-FH1, Notkestraße 85, 22607 Hamburg, Germany.

The process $eP \to eP\gamma$ has been investigated by both the H1 and ZEUS collaborations at HERA. Contributions beyond the normal QED Bethe-Heitler process have been seen within the measurable kinematic range. These contributions are consistent with a calculation of Deeply Virtual Compton Scattering. A cross section, differential in Q^2 or W, has been measured by the H1 collaboration and compared with this calculation.

1. Introduction

The study of exclusive final states in diffractive events at HERA has been used to aid our understanding of the underlying process. However, uncertainties in the probabilities of rapidity gap survival with jets or in the final state wave functions of vector mesons has created a constant trade-off between the ease of theoretical calculation and the ability to isolate the events experimentally. Recently, the exclusive production of real photons ($eP \to eP\gamma$) has received increased attention due to its clean final state for experimental observation and its well defined wave function for theoretical calculation.

2. Theoretical Considerations

The production of a real photon event with a rapidity gap has been calculated with two different approaches. Frankfurt, Freund and Strikman[1] (FFS) have calculated the cross-section for a two gluon exchange process (Fig. 1 left) that would create this final state. In their calculation, the Q^2 of the incoming virtual photon provides the evolution scale for the calculation and the proton is scattered elastically. Thus, their calculations are valid for kinematic regions where the squared four-momentum transfer to the proton ($|t|$) is low (less than a few GeV^2) and the Q^2 is high (greater than 4-6 GeV^2).

On the other hand, Evanson and Forshaw[2] have investigated a BFKL type calculation of real photon production. Such a calculation requires high $|t|$ (greater than 10 GeV^2) to provide the evolution scale of the gluon ladder (see Fig. 1 right). In addition, their calculations have been made with Q^2 close to zero.

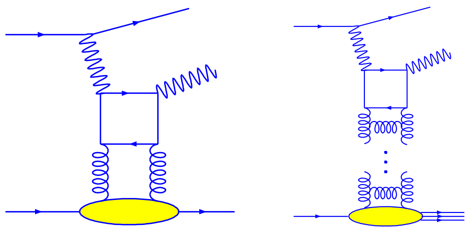

Figure 1. Fundamental diagrams of the QCD processes calculated to contribute to the reaction $eP \to eP\gamma$.

Preliminary experimental data from both the H1 and ZEUS collaborations for this event topology are now available primarily in the range of $2 < Q^2 < 10$ GeV^2 and elastic scattering off the proton ($|t| < 2$ GeV^2). This combination is in an unfavorable region for both theoretical approaches. However, since there is some overlap with the valid kinematic region used by FFS, calculations based on their work will be compared to the experimental data presented in this paper.

3. Backgrounds and Interference

The primary production mechanism for real photons is the Bethe-Heitler or QED Compton

*On behalf of the H1 and ZEUS Collaborations

†present address: Argonne National Lab, HEP Division, 9700 S. Cass Ave., Argonne, IL 60439

process (Fig. 2). In fact, the QED and QCD

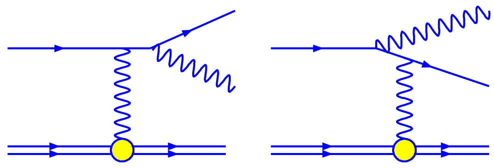

Figure 2. Diagrams of the Bethe-Heitler or QED Compton process.

processes are expected to interfere. This interference, which is included in the calculations of FFS and should by experimentally separable, may in the future allow access to interesting additional physics such as the skewed parton distribution of the proton.

The Bethe-Heitler process is most dominant at low $|t|$ and low Q^2. Therefore, the electron and photon from such events are both expected to be in the backward (small scattering angle) area of the detector and balanced in ϕ[‡]. Conversely, in the QCD processes described above, the electron scattering angle (θ) is directly related to Q^2 and therefore primarily expected to be backward. The photon, however, should have a relatively equal probability to be found in all θ ranges. Thus, to improve the ratio of QCD events to the QED background, both the H1 and ZEUS collaborations have selected event samples with an electron identified in the backward direction and a photon identified more centrally (See Table 1). In addition, any non-zero $|t|$ of the event should translate to an imbalance in the respective ϕ scattering angles of the two products, providing an additional discrimination possibility.

In addition to other photon production processes, there has been concern over possible background processes which could produce neutral hadrons (π^0 or η^0) that then decay into final state photons. The ZEUS collaboration has performed studies of cluster shapes and distributions[3] for photons from neutral hadrons and has concluded that the observed events are not consistent with such events. In addition, the finer granularity of the H1 detector allows the direct reconstruction of neutral hadron decay products for $p_{T_{(hadron)}} \leq 3$ GeV [4]. Since the observed photons are primarily at $p_T \sim 1-4$ GeV, contamination from any neutral hadrons is kept minimal by vetoing on any additional clusters above 500 MeV.

[‡]H1 and ZEUS use a cylindrical coordinate system with the origin at the interaction point and the positive z-axis defined as the proton beam direction

4. Event Detection

Both H1 and ZEUS have performed preliminary investigations into the data taken at HERA during 1996 and 1997. These runs, performed with 27.5 GeV positrons and 820 GeV protons, yielded 37 pb^{-1} of data for ZEUS and 8 pb^{-1} for H1. Similar event selections, described in Table 1, were used. An event with exactly two electromagnetic clusters was selected if it satisfied the given criteria. In addition, the central cluster was identified as a photon candidate by the exclusion of all tracks in the central detectors. To insure that these events were primarily elastic, no additional activity in the main calorimeter or forward detectors was allowed.

Table 1
Event selection criteria for H1 and ZEUS

	ZEUS	H1
Backward Candidate	$\theta > 160°$ $E > 10$ GeV	$\theta > 155°$ $E > 15$ GeV
Central Candidate	$\theta < 137°$ $E > 2$ GeV	$\theta < 142°$ $p_T > 1$ GeV
Kinematic Cuts	$Q^2 > 6\ \text{GeV}^2$ $\|\theta_1 - \theta_2\| > 45°$	$2 < Q^2 < 20\ \text{GeV}^2$ $30 < W < 120$ GeV $\|t\| < 1\ \text{GeV}^2$

In Figure 3, uncorrected detector distributions from the H1 event sample are shown. These are compared with the Compton 2.0[5] Monte Carlo, also on detector level and normalized to luminosity, which has been confirmed to accurately describe the Bethe-Heitler process at HERA kinematics. It is apparent that, in addition to normalization differences, the shapes of the distributions are significantly different, indicating the existence of a different process. In particular, the relatively flat θ distribution of the LAr clusters compared

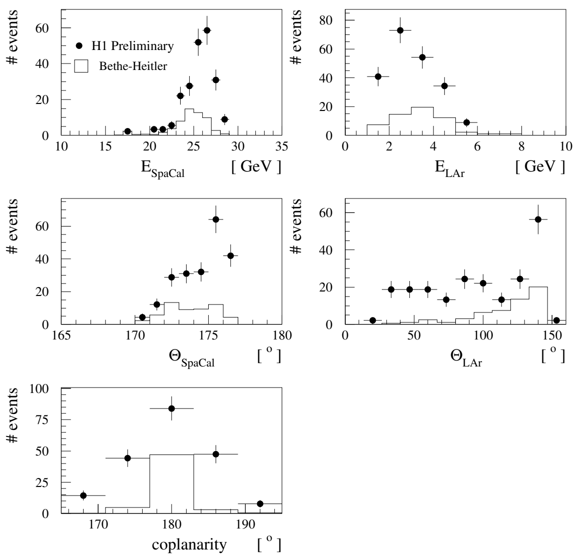

Figure 3. Uncorrected kinematic distributions of signal events in H1 compared with the Compton 2.0 Monte Carlo. Events require an identified electron in the *SpaCal* ($\theta > 155°$) and an identified photon in the *LAr* ($\theta < 142°$). The coplanarity refers to the difference in ϕ between the electron and photon candidates.

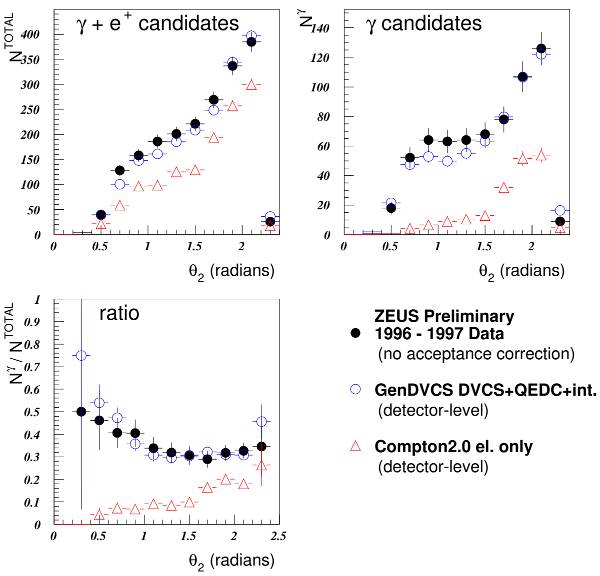

Figure 4. Uncorrected kinematic distributions of signal events in ZEUS compared with the Compton 2.0 and GenDVCS Monte Carlos. Events require two identified clusters. θ_2 refers to the more forward of the two candidates ($\theta < 137°$). Positron and photon candidates are differentiated by the existence of a linked track to the cluster.

with the rapidly falling Monte Carlo shows exactly the expected behavioral difference between the QED and QCD processes.

The ZEUS data, also on detector level (see Fig. 4), show this same effect. In addition to the Compton 2.0 Monte Carlo, the ZEUS data for the scattering angle of the most forward cluster (θ_2) are compared to a Monte Carlo implementation of the equations presented by FFS. This Monte Carlo has been compared on detector level and only normalized to luminosity. One can see quite rapidly that the detector distributions and shapes are much better described than by the Compton Monte Carlo alone.

5. Cross Section Measurement

To create a differential cross section measurement, the H1 collaboration have corrected the data for detector acceptances and trigger efficiencies. In addition, contributions from initial state radiation and undetected proton dissociation have been calculated and subtracted. Figure 5 shows the differential cross section as a function of Q^2. Both statistical and systematic errors are shown. The systematic error contributions are dominated by the acceptance corrections (10%), the angular resolution (5-10%), and the dissociative background subtraction (5%).

These data contain contributions from both the QED and QCD processes. The expected contribution from the Bethe-Heitler process, as calculated by Compton 2.0, is shown in the hatched region. It clearly falls below the measured cross section by about a factor of 5. In addition, the lightly shaded region shows the results of a Monte Carlo calculation based on the work of FFS. This Monte Carlo includes contributions from the QED, QCD, and interference processes. The agreement is seen to be very good, even down to $Q^2 \sim 2$ GeV^2, below it's expected applicabil-

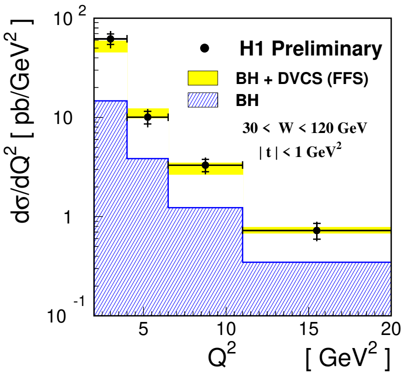

Figure 5. Differential cross section as a function of Q^2 for the process $eP \rightarrow eP\gamma$. Statistical (inner) and systematic (outer) errors are shown. The hatched region corresponds to the calculation of the Bethe-Heitler process by the Compton 2.0 Monte Carlo. The lightly shaded region shows the results of a calculation based on [1] with the $|t|$ dependence varied between 7-10 GeV^{-2}.

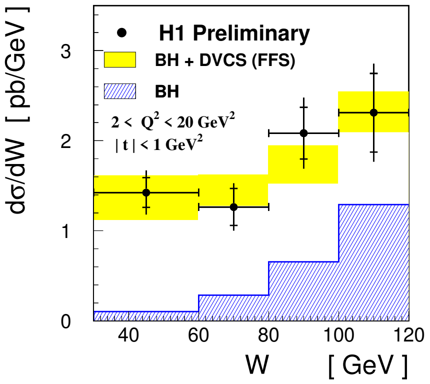

Figure 6. Differential cross section as a function of W for the process $eP \rightarrow eP\gamma$. Statistical (inner) and systematic (outer) errors are shown. The hatched region corresponds to the calculation of the Bethe-Heitler process by the Compton 2.0 Monte Carlo. The lightly shaded region shows the results of a calculation based on [1] with the $|t|$ dependence varied between 7-10 GeV^{-2}.

ity. The range of the lightly shaded region corresponds to variation of the assumed $|t|$ dependence of the DVCS process in the Monte Carlo calculation between 7 - 10 GeV^{-2}.

In Figure 6, the differential cross section is shown in bins of W. Here, the very different, almost flat, shape can be clearly seen relative to the underlying QED calculation. Again the calculations based on FFS seem to be in agreement with the data.

6. Final Comment

Both H1 and ZEUS have separately implemented the equations of FFS into Monte Carlo generators. Both programs have been cross checked and are in agreement. Therefore, the agreement with the data is a significant sign of the observation of a QCD process in this final state. However, it is apparent that the $|t|$ dependence of this DVCS process has a large effect on the overall normalization of the calculated cross section. At this time, there exists no preferred value for this dependence. The shown values were inferred from previous measurements of diffractive ρ production. Similarly, the effect of proton dissociation was also assumed to be consistent with that measured in elastic ρ production. It is hoped that additional statistics will allow a direct measurement of some of these parameters, thus aiding the final understanding of this process.

It is significant to note, however, that despite these uncertainties, contributions from a non-QED process have been seen to contribute to the process $eP \rightarrow eP\gamma$. In addition, the Q^2 evolution of this process is seen to be consistent with the calculations of FFS which are based on a 2 gluon exchange model.

REFERENCES

1. L.L.Frankfurt, A.Freund and M.Strikman, Phys. Rev. D58, 114001 (1998); Phys. Rev. D59, 119901E (1999).
2. N.G.Evanson and J.R.Forshaw, Phys. Rev. D60, 34016 (1999).
3. ZEUS Collaboration, Phys. Lett. B472, 175 (2000).
4. H1 Collaboration, DESY-00-085, *accepted by Eur. Phys. J. C (2000).*
5. A.Courau and P.Kessler, Phys. Rev. D46, 117 (1992).